HHS Public Access

Author manuscript

Amyotroph Lateral Scler Frontotemporal Degener. Author manuscript; available in PMC 2019 November 01.

Published in final edited form as:

Amyotroph Lateral Scler Frontotemporal Degener. 2018 November ; 19(7-8): 562–569. doi: 10.1080/21678421.2018.1517180.

Loss of functional connectivity is an early imaging marker in primary lateral sclerosis

Michael G. Clark, BS, **Rachel Smallwood Shoukry, PhD**, **Caleb J. Huang, BS**, **Laura E. Danielian, MS**, **Devin Bageac, BS**, and **Mary Kay Floeter, MD PhD***

National Institute of Neurological Disorders and Stroke, National Institutes of Health, 10 Center Drive MSC 1140, Bethesda MD 20892-1140, USA

Abstract

Objective: The clinical diagnosis of primary lateral sclerosis can only be made after upper motor neuron symptoms have progressed for several years without developing lower motor neuron signs. The goal of the study was to identify neuroimaging changes that occur early in primary lateral sclerosis, prior to clinical diagnosis.

Methods: MRI scans were obtained on 13 patients with adult-onset progressive spasticity for five years or less who were followed longitudinally to confirm a clinical diagnosis of primary lateral sclerosis. Resting state functional MRI, diffusion tensor imaging, and anatomical images were obtained. These 'pre-PLS' patients were compared to 18 patients with longstanding, established primary lateral sclerosis and 28 controls.

Results: Pre-PLS patients had a marked reduction in seed-based resting-state motor network connectivity compared to controls and patients with longstanding disease. White matter regions with reduced fractional anisotropy were similar in the two patient groups compared to controls. Patients with longstanding disease had cortical thinning of the precentral gyrus. A slight thinning of right precentral gyrus was detected in initial pre-PLS patients' scans. Follow-up scans in 8 pre-PLS patients 1-2 years later showed increasing motor connectivity, thinning of the precentral gyrus, and no change in diffusion measures of the corticospinal tract or callosal motor region.

Conclusions: Loss of motor functional connectivity is an early imaging marker in primary lateral sclerosis. This differs from literature descriptions of amyotrophic lateral sclerosis, warranting further studies to test whether resting-state functional MRI can differentiate between amyotrophic lateral sclerosis and primary lateral sclerosis at early disease stages.

Keywords

Primary lateral sclerosis; imaging; functional connectivity

*Corresponding author: Mary Kay Floeter MD PhD, Phone 301-496-9957, Fax 301-451-9805, floeterm@ninds.nih.gov.

Declaration of Interest

The authors have no conflicts of interest to disclose

Introduction

Primary lateral sclerosis (PLS) is a motor neuron disease variant characterized by the insidious onset of progressive spasticity caused by degeneration of corticospinal neurons (1). PLS patients survive more than a decade after symptom onset (2, 3) but the rate of progression is most rapid in the first years after symptoms begin, often reaching a plateau after seven to eight years (4). This clinical course suggests a limited time window during which corticospinal neurons degenerate and when potential interventions should be targeted. Unfortunately, the diagnosis of PLS is based on clinical criteria that require symptoms to be present for 3-5 years without development of lower motor neuron signs (5, 6). In the first several years of symptoms, clinical signs alone do not allow distinction between PLS and patients who subsequently develop amyotrophic lateral sclerosis (ALS) (2, 7).

Neuroimaging findings in patients with long-standing PLS include atrophy of the motor cortex (8, 9), white matter changes in the corticospinal tract and corpus callosum (10–13), and changes in resting-state networks (14, 15). Neuroimaging changes that occur in the first years after symptoms begin, before the diagnosis can be made, are unknown. We hypothesized that functional changes would occur at early stages of disease. To test this hypothesis, we prospectively scanned successive patients with progressive spasticity for less than five years who were suspected to have PLS and followed them clinically. We report here the findings on 13 patients who met criteria for clinically pure PLS (3) after five years of symptoms. This cohort of ‘pre-PLS’ patients was compared to ‘established’ PLS patients and healthy controls.

Materials and Methods

Subjects

All participants gave written, informed consent for the protocols in accord with the Declaration of Helsinki and the Institutional Review Board. Between Sept 2012 and June 2016 three groups of participants were scanned. The ‘pre-PLS’ group consisted of successive patients referred during this period for evaluation of possible PLS with symptoms for five years or less and who subsequently met criteria for clinical PLS after clinical follow-up beyond five years of symptoms. The ‘established PLS’ group had more than five years of progressive upper motor neuron symptoms. The third group consisted of healthy controls. All patients and controls had neurological examinations, measures of finger tapping rates, 9-hole peg test times, and the Mini-mental state exam (MMSE) (16). All healthy controls had normal neurological examinations and MMSE scores. None of the PLS and pre-PLS patients had MMSE scores indicative of dementia. All pre-PLS patients and established PLS patients had an EMG after five years of symptoms that showed no acute denervation. None of the participants had a family history of ALS, PLS, or frontotemporal dementia.

MRI acquisition and processing

All participants were scanned on a single 3T MRI scanner (GE HDX, GE Medical Systems, Milwaukee, WI) with a receive-only, eight-channel head coil. The acquisition sequences and processing methods are described briefly below and in detail in Supplemental material 1,

and in previous publications (17). The acquisition sequences consisted of 1) two high-resolution T1-weighted sequences that were averaged at each time point for FreeSurfer evaluation of volumes and cortical thickness; 2) resting-state functional MRI (rs-fMRI) with visual fixation; 3) a finger tapping task fMRI, alternating 20-s blocks of finger tapping with 30-s blocks of rest, each hand tested separately; 4) multi-slice diffusion weighted images with a total of 80 diffusion volumes including 70 directions of gradient, with 10 volumes at b=300 s/mm^2 and 60 volumes at b=1100 s/mm^2, and 10 additional (b0) volumes; 5) a high-resolution T2-weighted image for anatomical registration and echo-planar distortion correction. Table 1 shows the number of participants with technically adequate studies for each MRI modality. Eight Pre-PLS patients returned for repeat scans approximately one year later, and four of those patients had a third scan the following year.

Finger-tapping fMRI data were pre-processed and analyzed using FSL's FEAT Version 6.00 (FMRIB's Software Library, www.fmrib.ox.ac.uk/fsl). Left- and right-hand finger tapping data from the healthy volunteers were analyzed separately to determine the MNI coordinates of the voxel of peak activation during each task. These voxels were then used as the center of 10-mm diameter motor Volumes of Interest (VOIs) in each individual's functional space for seed-based functional connectivity. Preprocessing of the resting-state fMRI data was also performed with FSL and included motion and slice timing correction, spatial smoothing, high pass filtering, regression to remove effects of nuisance variables, low-pass filtering (0.1 Hz) and normalization. A whole-brain seed-voxel correlation analysis was performed for each subject with their motor VOI. FMRIB's Local Analysis of Mixed Effects (FSL FLAME) was used for group-level comparison of correlation maps, and the resulting Z-statistic images were thresholded using clusters determined by $Z > 2.0$ and a (corrected) cluster significance threshold of $P \leq 0.05$ (18). Age and gender were included as covariates, and all pair-wise group contrasts were evaluated. Longitudinal motor seed functional connectivity changes across two time points in the pre-PLS group were evaluated using a repeated measures ANOVA, applying the same statistical thresholds as above. For the four pre-PLS patients with two follow-up scans, the last scan was used.

Cortical reconstruction and volumetric segmentation was performed with the FreeSurfer image analysis suite (http://surfer.nmr.mgh.harvard.edu/). All images were visually inspected by two investigators and errors in segmentation were manually corrected. The tessellated surfaces were inflated and registered to the Desikan-Killiany atlas which parcellates the cerebral cortex into 34 regions in each hemisphere based on gyral and sulcal structures (19). The mean thickness of the precentral and postcentral regions was assessed at baseline for all participants. The FreeSurfer longitudinal stream (20) was used for processing pre-PLS patients with multiple scans for measures of precentral gyrus thickness.

The diffusion tensor images (DTI) were processed using the TORTOISE software package (https://science.nichd.nih.gov/confluence/display/nihpd/TORTOISE), including calculation of the tensor and metrics of fractional anisotropy (FA), mean diffusivity (MD), axial diffusivity (AD) and radial diffusivity (RD). A voxel-wise comparison of whole-brain FA skeletons of the pre-PLS, established PLS, and control groups was carried out in Tract-Based Spatial Statistics (TBSS v1.2, http://www.fmrib.ox.ac.uk/fsl/) (21), with gender and age as covariates, using Threshold-Free Cluster Enhancement and family-wise error

correction for multiple comparisons with $p < 0.05$ as threshold for significance. Whole-tract diffusion metrics were obtained for the corticospinal tract using fiber tracking methods previously described (22) and for segments of the corpus callosum as defined by Hofer and Frahm (23).

Statistics

Results are reported as mean ± standard deviation in Tables and text. Shapiro Wilk tests were used to evaluate normality for clinical and demographic values. ANOVA with Tukey's post-hoc testing was used to compare age. Kruskal-Wallis with Dunn's post-hoc testing was used to compare other clinical and demographic variables, with Mann-Whitney testing to compare pre-PLS with established PLS. Multivariate analysis was used to compare cortical thickness between the three diagnostic groups, including age, gender and education as covariates, and Bonferroni correction for post-hoc comparisons (IBM SPSS v.25). ANOVA with Tukey's post-hoc testing was used to compare fiber tracking measures between patients and controls. The relationship between diffusion tensor indices and connectivity of the seeds used for functional connectivity was assessed using multiple regression. Significance threshold was $p < 0.05$ (corrected).

Results

Demographics

Clinical and demographic data are shown in Table 1. The Pre-PLS cohort consisted of thirteen patients referred for suspected PLS with symptoms of spasticity for less than five years, who continued to have a pure upper motor neuron syndrome during clinical follow-up beyond five years. Symptom duration at baseline was 3.2 ± 1.3 years (range 1.5-5 years) and the clinical follow-up period was 3.3 ± 1.3 years. Eight patients had a follow-up scan (1.1 ± 0.4 years after baseline scan) and four patients had a third scan (2.6 ± 0.7 years after baseline scan). The established PLS cohort consisted of 18 PLS patients whose symptom duration exceeded five years (13.3 ± 7.6 years) seen during the same time period. There was no difference in the age of symptom onset between the established PLS group and pre-PLS group. Although the pre-PLS group was slightly younger than the established PLS group, the age difference between patient groups was not statistically significant. Symptoms began in the legs in the majority of patients in both groups, as shown in Table 1. The healthy control group consisted of twenty-eight healthy controls scanned during the same time period. The mean age of controls was intermediate between the two patient groups, younger than the established PLS group but not significantly different from the pre-PLS group. These healthy controls also participated in a previously reported study (24). Finger tapping rates and peg-task measures were reduced in PLS and pre-PLS groups compared to controls. PLS and pre-PLS groups had similar ALSFRS-R scores and finger-tapping rates, but dexterity on a right-hand peg-test task was worse in established PLS patients. The number of participants in each group with technically adequate scans is shown for each imaging modality in Table 1.

Resting-state fMRI

Analysis of the right- and left-hand finger tapping task fMRIs revealed voxels of peak activation in the left and right motor cortex, respectively. Spherical VOIs used to generate the motor resting-state network were constructed such that they were centered around these voxels. (**bottom center,** Figure 1). Pre-PLS patients had markedly reduced functional connectivity of the right motor cortex seed in a whole brain analysis compared to controls (Figure 1A). Regions with reduced connectivity to the right motor cortex seed included the bilateral postcentral gyri, supplemental motor areas, cuneus, and the contralateral inferior parietal lobule, occipital lobe, and superior and inferior temporal gyri. Established PLS patients did not significantly differ from controls. Compared to pre-PLS patients, established PLS patients had greater connectivity of the right motor cortex seed to the contralateral precentral gyrus, postcentral gyrus, and middle/inferior temporal gyri (Figure 1B). Connectivity of the left motor cortex seed was also reduced in pre-PLS patients compared to controls in a similar pattern to the right seed (results not shown).

In the eight pre-PLS patients who had follow-up scans, changes in motor connectivity were assessed by comparing each patient's first and last scan (4 with 1-year follow-up; 4 with 2-year follow-up). Regions that showed increased connectivity to the right motor cortex seeds included the bilateral frontal and parieto-occipital cortices and the left cerebellum (Figure 1C). Regions with increased connectivity to the left motor cortex seed included bilateral frontal cortex and the the left parieto-occipital region (not shown).

Cortical Thickness and volumes

Established PLS patients had bilateral thinning of the precentral cortex compared to controls (Figure 2A). The pre-PLS patients had mild thinning of the right precentral gyrus at baseline compared to controls (Figure 2A). There was no difference in the thickness of the postcentral gyrus in the three groups (Figure 2B). In pre-PLS patients who had follow-up scans, there was a gradual decline in precentral gyrus thickness (Figure 2C, D**)**.

White matter

The whole-brain analysis of DTI white matter skeletons showed that pre-PLS and established PLS patients both differed from controls, with reduced FA and increased MD in the corticospinal tract and corpus callosum (Figure 3). Regions of affected white matter were not significantly different between pre-PLS and established PLS groups ($p < 0.05$, FWE correction, not shown). Fiber tracking showed reduced FA and increased radial diffusivity in the CST bilaterally and the motor segment of the corpus callosum in both patient groups compared to controls (Supplemental Table), but no difference in CST FA between Pre-PLS and PLS patients. The right CST MD was increased in both groups, and the left CST MD was increased in established PLS patients. MD was increased in the motor segment of the callosum in both groups compared to controls. MD of the genu and premotor segment of the callosum was significantly greater in established PLS patients compared to controls. MD of the premotor and AD of the motor segment of the callosum were greater in established PLS patients than pre-PLS patients, with a trend toward increased MD in the motor segment ($p = 0.08$). There were no differences in RD between pre-PLS and established PLS patients. Multiple regression analysis showed that the FA of the three tracts originating from the

motor cortices (right and left CST, motor segment of the corpus callosum) were weak predictors of the connection strength between finger tapping seeds used for generating the motor network (R=0.464, p = 0.013). Diffusion measures of the splenium did not differ from controls. In the eight pre-PLS patients with longitudinal scans, diffusion measures of the corticospinal tract and motor segment of the callosum qualitatively showed little change over time (Supplemental Figure).

Discussion

We prospectively followed a cohort of patients with less than five years of pure upper motor neuron dysfunction to identify early neuroimaging findings in primary lateral sclerosis. The most striking finding in this cohort of pre-PLS patients was the loss of connectivity to a seed in the motor cortex in resting-state functional MRI scans. Pre-PLS patients also had evidence for reduced integrity of white matter within the motor segment of the corpus callosum and the corticospinal tract in diffusion tensor images. The temporal relationship between reduced white matter integrity and the functional disconnection of the primary motor cortex from the rest of the brain at the earliest stage of disease will require further study since fMRI and DTI findings were both present in this cohort at the time of the first scan. White matter changes and the loss of functional connectivity precede atrophy and thinning of the motor cortex as seen in the cohort of PLS patients with longstanding symptoms. Thinning of the precentral cortex occurred over time in pre-PLS patients followed longitudinally.

In our cross-sectional analysis, the decreased motor functional connectivity in the first years after symptoms begin appears to be followed by a degree of recovery in patients with longstanding PLS. In the longitudinal analysis of the eight pre-PLS patients with scans at two timepoints, increased motor connectivity was not accompanied by changes in diffusion measures of callosal or corticospinal tracts, arguing against axonal regrowth as the mechanism. The return of motor connectivity is consistent with two previous studies suggesting that some functional re-organization occurs over time in PLS patients (14, 15, 25). One previous study using independent components analysis (ICA) showed that functional connectivity in sensorimotor networks was greater in PLS patients than controls (15). Although our study found that motor connectivity was greater in the established PLS group than the pre-PLS group, it did not show greater motor connectivity in established PLS patients than in controls. Differences in methods can account for this discrepancy. To generate the network, we used a small, focal region of the precentral gyrus that was activated by finger-tapping as a seed, and assessed the temporal correlation of blood-oxygen dependent levels in this seed with other cortical regions of the brain. This contrasts with ICA and data-driven methods, which delineate spatial components with correlated time courses from the whole brain (26). Although the resulting ICA component maps may be generally similar to the seed-based map, ICA maps tend to encompass larger regions of brain and are less specific to the brain region of interest. We chose the precentral seed for its anatomical and clinical relevance; PLS is known to cause focal atrophy of the precentral gyrus, and both pre-PLS and established PLS patients had impaired clinical measures of finger tapping and dexterity.

Previous studies report that structurally connected brain regions are functionally connected (27). The motor cortices are connected by callosal fibers, which mediate interhemispheric inhibition. The strength of interhemispheric inhibition is correlated with fractional anisotropy of the callosal fibers connecting the primary motor cortices (28). Interhemispheric inhibition promotes unilateral activation of the motor cortex activation during unimanual motor tasks (29). In pre-PLS patients, loss of callosal connections could partly explain the early decline in motor connectivity, but the mechanism underlying increased motor connectivity over time is uncertain. Repair of callosal connections is unlikely because even established PLS patients have reduced fractional anisotropy of callosal fibers (12, 15). Increased functional connectivity in PLS could result from loss of cortical inhibitory interneurons, as has been hypothesized for ALS (30, 31). Reduction of cortical inhibitory interneuron activity would be predicted to cause broader, less refined activation of cortical microcircuits during movement and to cause mirror movements (32). Although it is speculative to extrapolate task-related activation patterns from resting state patterns in PLS, it has been shown that increased resting state sensorimotor functional connectivity increases in aging (33–35) and is inversely correlated with motor performance in aged adults (34). In PLS, increased motor connectivity may result from degradation of selective activation signals rather than a compensatory mechanism to improve motor performance.

The early loss of motor functional connectivity in the present study suggests that functional imaging changes may be detectable before patients meet clinical criteria for PLS that require symptoms to be present for 3-5 years without development of lower motor neuron signs (5, 6). However, the findings in this study are based on a relatively small sample of patients and should be considered preliminary. This limitation reflects the rarity of PLS, which accounts for only a small percentage of patients in ALS clinics (2). The lack of an ALS cohort for comparison reflects a limitation of our clinic, which was established for studying PLS. A prospective study of newly-presenting ALS clinic patients is needed to test whether resting-state functional MRI can differentiate between ALS and pre-PLS patients in the first years after symptom onset.

Supplementary Material

Refer to Web version on PubMed Central for supplementary material.

Acknowledgements

The study was funded by the Intramural Research Program of the National Institute of Neurological Disorders and Stroke, NIH, Z01 NS002976. Protocols are registered on www.clinicaltrials.gov (NCT00015444 and NCT01517087). This work utilized the computational resources of the NIH HPC Biowulf cluster (http://hpc.nih.gov).

References

1. Statland JM, Barohn RJ, Dimachkie MM, Floeter MK, and Mitsumoto H, Primary Lateral Sclerosis. Neurol Clin, 2015 33(4): p. 749–60. [PubMed: 26515619]
2. Tartaglia MC, Rowe A, Findlater K, Orange JB, Grace G, et al., Differentiation between primary lateral sclerosis and amyotrophic lateral sclerosis: examination of symptoms and signs at disease onset and during follow-up. Arch Neurol, 2007 64(2): p. 232–6. [PubMed: 17296839]

3. Gordon PH, Cheng B, Katz IB, Pinto M, Hays AP, et al., The natural history of primary lateral sclerosis. Neurology, 2006 66(5): p. 647–53. [PubMed: 16534101]
4. Floeter MK and Mills R, Progression in primary lateral sclerosis: a prospective analysis. Amyotroph Lateral Scler, 2009 10(5-6): p. 339–46. [PubMed: 19922121]
5. Pringle CE, Hudson AJ, Munoz DG, Kiernan JA, Brown WF, et al., Primary lateral sclerosis. Clinical features, neuropathology and diagnostic criteria. Brain, 1992 115(Pt 2): p. 495–520. [PubMed: 1606479]
6. Singer MA, Statland JM, Wolfe GI, and Barohn RJ, Primary lateral sclerosis. Muscle Nerve, 2007 35(3): p. 291–302. [PubMed: 17212349]
7. Gordon PH, Cheng B, Katz IB, Mitsumoto H, and Rowland LP, Clinical features that distinguish PLS, upper motor neuron-dominant ALS, and typical ALS. Neurology, 2009 72(22): p. 1948–52. [PubMed: 19487653]
8. Kwan JY, Meoded A, Danielian LE, Wu T, and Floeter MK, Structural imaging differences and longitudinal changes in primary lateral sclerosis and amyotrophic lateral sclerosis. Neuroimage 2012 2: p. 151–60. [PubMed: 24179768]
9. Tartaglia MC, Laluz V, Rowe A, Findlater K, Lee DH, et al., Brain atrophy in primary lateral sclerosis. Neurology, 2009 72(14): p. 1236–41. [PubMed: 19349603]
10. Kolind S, Sharma R, Knight S, Johansen-Berg H, Talbot K, et al., Myelin imaging in amyotrophic and primary lateral sclerosis. Amyotroph Lateral Scler Frontotemporal Degener, 2013.
11. Menke RA, Abraham I, Thiel CS, Filippini N, Knight S, et al., Fractional anisotropy in the posterior limb of the internal capsule and prognosis in amyotrophic lateral sclerosis. Arch Neurol, 2012 69(11): p. 1493–9. [PubMed: 22910997]
12. Iwata NK, Kwan JY, Danielian LE, Butman JA, Tovar-Moll F, et al., White matter alterations differ in primary lateral sclerosis and amyotrophic lateral sclerosis. Brain, 2011 134(Pt 9): p. 2642–55. [PubMed: 21798965]
13. Filippini N, Douaud G, Mackay CE, Knight S, Talbot K, et al., Corpus callosum involvement is a consistent feature of amyotrophic lateral sclerosis. Neurology, 2010 75(18): p. 1645–52. [PubMed: 21041787]
14. Meoded A, Morrissette AE, Katipally R, Schanz O, Gotts SJ, et al., Cerebro-cerebellar connectivity is increased in primary lateral sclerosis. Neuroimage Clin, 2015 7: p. 288–96. [PubMed: 25610792]
15. Agosta F, Canu E, Inuggi A, Chio A, Riva N, et al., Resting state functional connectivity alterations in primary lateral sclerosis. Neurobiol Aging, 2014 35(4): p. 916–25. [PubMed: 24211007]
16. Folstein MF, Folstein SE, and McHugh PR, "Mini-mental state". A practical method for grading the cognitive state of patients for the clinician. J Psychiatr Res, 1975 12(3): p. 189–98. [PubMed: 1202204]
17. Sarlls JE, Pierpaoli C, Talagala SL, and Luh WM, Robust fat suppression at 3T in high-resolution diffusion-weighted single-shot echo-planar imaging of human brain. Magn Reson Med, 2011 66(6): p. 1658–65. [PubMed: 21604298]
18. Worsley KJ, Statistical analysis of activation images, in Functional MRI: An Introduction to Methods, Jezzard P, Matthews PM, and Smith SM, Editors. 2001.
19. Desikan RS, Segonne F, Fischl B, Quinn BT, Dickerson BC, et al., An automated labeling system for subdividing the human cerebral cortex on MRI scans into gyral based regions of interest. Neuroimage, 2006 31(3): p. 968–80. [PubMed: 16530430]
20. Reuter M, Schmansky NJ, Rosas HD, and Fischl B, Within-subject template estimation for unbiased longitudinal image analysis. Neuroimage, 2012 61(4): p. 1402–18. [PubMed: 22430496]
21. Smith SM, Jenkinson M, Johansen-Berg H, Rueckert D, Nichols TE, et al., Tract-based spatial statistics: voxelwise analysis of multi-subject diffusion data. Neuroimage, 2006 31(4): p. 1487–505. [PubMed: 16624579]
22. Danielian LE, Iwata NK, Thomasson DM, and Floeter MK, Reliability of fiber tracking measurements in diffusion tensor imaging for longitudinal study. Neuroimage, 2010 49(2): p. 1572–80. [PubMed: 19744567]

23. Hofer S and Frahm J, Topography of the human corpus callosum revisited--comprehensive fiber tractography using diffusion tensor magnetic resonance imaging. Neuroimage, 2006 32(3): p. 989–94. [PubMed: 16854598]
24. Floeter MK, Bageac D, Danielian LE, Braun LE, Traynor BJ, et al., Longitudinal imaging in C9orf72 mutation carriers: Relationship to phenotype. Neuroimage Clin, 2016 12: p. 1035–1043. [PubMed: 27995069]
25. Proudfoot M, Colclough GL, Quinn A, Wuu J, Talbot K, et al., Increased cerebral functional connectivity in ALS: A resting-state magnetoencephalography study. Neurology, 2018 90(16): p. e1418–e1424. [PubMed: 29661904]
26. Joel SE, Caffo BS, van Zijl PC, and Pekar JJ, On the relationship between seed-based and ICA-based measures of functional connectivity. Magn Reson Med, 2011 66(3): p. 644–57. [PubMed: 21394769]
27. van den Heuvel MP, Mandl RC, Kahn RS, and Hulshoff Pol HE, Functionally linked resting-state networks reflect the underlying structural connectivity architecture of the human brain. Hum Brain Mapp, 2009 30(10): p. 3127–41. [PubMed: 19235882]
28. Fling BW, Benson BL, and Seidler RD, Transcallosal sensorimotor fiber tract structure-function relationships. Hum Brain Mapp, 2013 34(2): p. 384–95. [PubMed: 22042512]
29. Tazoe T and Perez MA, Speed-dependent contribution of callosal pathways to ipsilateral movements. J Neurosci, 2013 33(41): p. 16178–88. [PubMed: 24107950]
30. Douaud G, Filippini N, Knight S, Talbot K, and Turner MR, Integration of structural and functional magnetic resonance imaging in amyotrophic lateral sclerosis. Brain, 2011 134(Pt 12): p. 3470–9. [PubMed: 22075069]
31. Maekawa S, Al-Sarraj S, Kibble M, Landau S, Parnavelas J, et al., Cortical selective vulnerability in motor neuron disease: a morphometric study. Brain, 2004 127(Pt 6): p. 1237–51. [PubMed: 15130949]
32. Sehm B, Steele CJ, Villringer A, and Ragert P, Mirror Motor Activity During Right-Hand Contractions and Its Relation to White Matter in the Posterior Midbody of the Corpus Callosum. Cereb Cortex, 2016 26(11): p. 4347–4355. [PubMed: 26400922]
33. Betzel RF, Byrge L, He Y, Goni J, Zuo XN, et al., Changes in structural and functional connectivity among resting-state networks across the human lifespan. Neuroimage, 2014 102 Pt 2: p. 345–57. [PubMed: 25109530]
34. Fling BW and Seidler RD, Fundamental differences in callosal structure, neurophysiologic function, and bimanual control in young and older adults. Cereb Cortex, 2012 22(11): p. 2643–52. [PubMed: 22166764]
35. He H, Luo C, Chang X, Shan Y, Cao W, et al., The Functional Integration in the Sensory-Motor System Predicts Aging in Healthy Older Adults. Front Aging Neurosci, 2016 8: p. 306. [PubMed: 28111548]

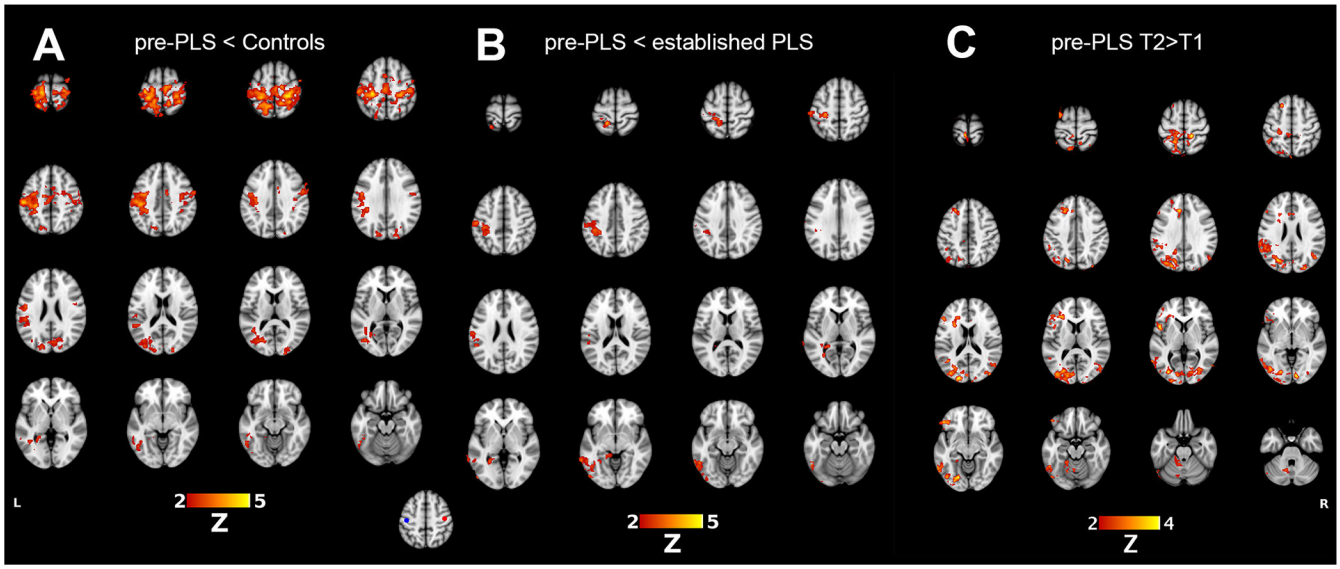

Figure 1.

Motor resting-state networks, showing differences in connectivity of the right motor cortex seed to the rest of the brain. (A) Red indicates brain regions with reduced connectivity in pre-PLS patients compared to heathy controls. (B) Red indicates brain regions in which established PLS patients have greater connectivity than in pre-PLS patients. (C) For eight pre-PLS patients with follow-up scans, regions in red had greater connectivity with the right motor cortex seed at the second timepoint (T2) compared to the first study (T1). Inset figure: 10-mm VOIs for generating the sensorimotor resting-state network were obtained from the voxel of peak activation in the left (MNI: −42, −20, 52; blue circle) and right (42, −16, 52; red circle) motor cortex from the right and left hand tapping task fMRI.

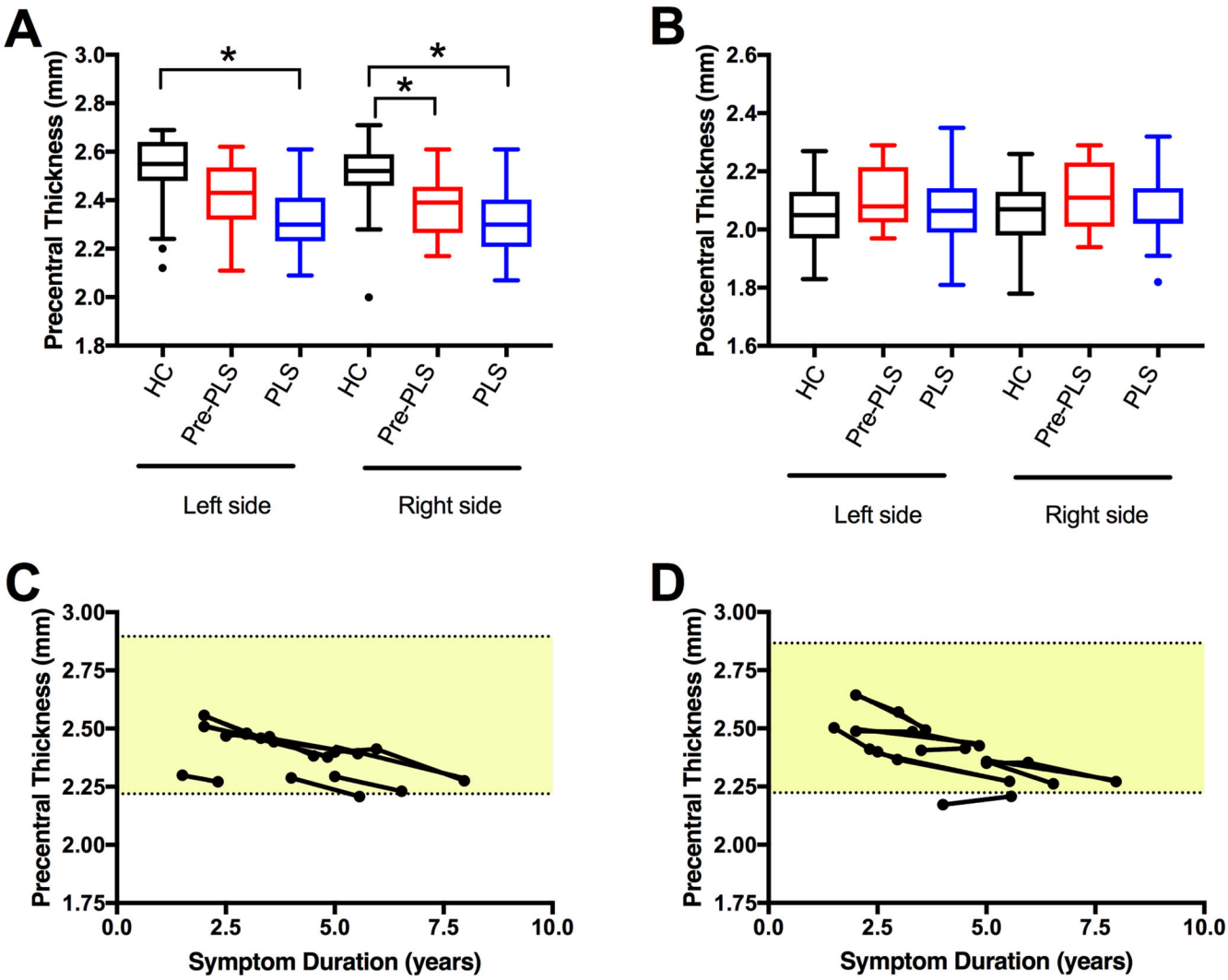

Figure 2.

Thinning of the motor cortex in PLS patients.

(A) The mean thickness of the precentral gyrus was reduced in both hemispheres in established PLS patients (blue) compared to healthy controls (HC, black). Slight thinning of the right precentral cortex was seen in pre-PLS patients (red) at baseline. Asterisks indicate Bonferroni-corrected $p < 0.05$. Age, gender, and education were included as covariates. (B) In contrast, the postcentral gyrus had no significant thinning in PLS and Pre-PLS patients. (C, D) Longitudinal measures of cortical thickness of the precentral gyrus of 8 pre-PLS patients who had repeated scans. Cortical thickness is plotted against years since symptom onset. (C) Left precentral gyrus and (D) right precentral gyrus. Shaded area indicates the range of thickness for the healthy controls (mean ± 2 SDs).

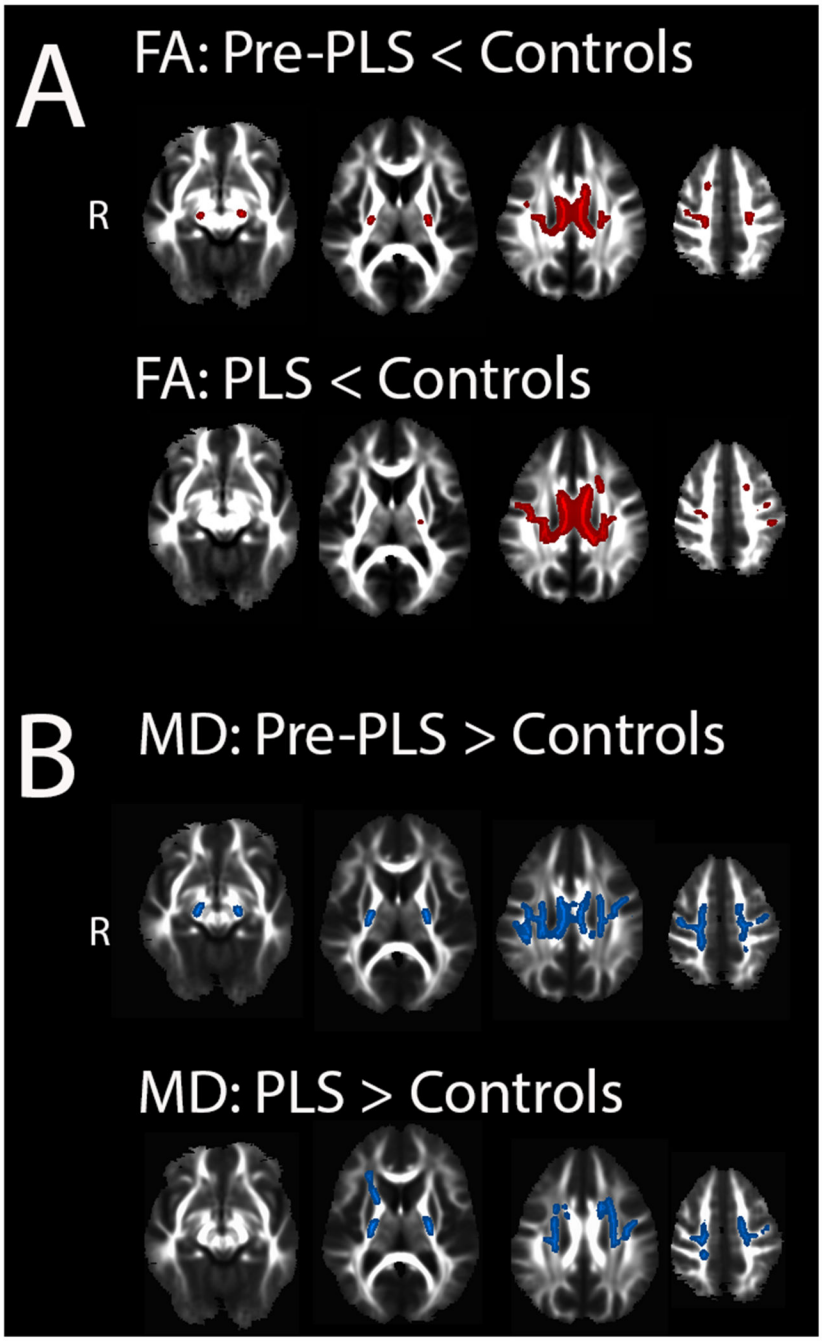

Figure 3.

White matter changes in patients compared to controls.

Regions of white matter with (A) reduced fractional anisotropy (red) in pre-PLS patients (top row) and established PLS patients (bottom row) compared to healthy controls. Regions of white matter with (B) increased mean diffusivity (blue) in pre-PLS patients (top row) and established PLS patients (bottom row) compared to healthy controls. There was no

significant difference between pre-PLS and PLS patients (Tract-based spatial statistics, $p < 0.05$, FWE corrected.)

Table 1.

Demographic and clinical data

	Healthy controls N=28	Pre-PLS N=13	Established PLS N=18
Age (yrs.)	52.8 ± 9.1	55.2 ± 6.5	62.7 ± 9.0[a]
Gender (M:F)	18:10	8:5	12:6
Age of symptom onset	-	50.7 ± 1.6	49.2 ± 2.2
Education (yrs)	16.3 ± 2.8	15.6 ± 2.5	15.8 ± 2.1
Symptom Duration (yrs.)	-	3.2 ± 1.3	13.3 ± 7.6[b]
Site of symptom onset Bulbar/upper extremity/leg	-	1/1/11	2/1/15
Dominant hand (R:L)	27:1	12:1	18:1
MiniMental State Exam	29.0 ± 1.2	29.3 ± 0.9	28.6 ± 1.6
ALSFRS-R score	-	39.8 ± 4.5	38.6 ± 4.0
Bulbar ALSFRS subscore	-	10.3 ± 2.0	9.5 ± 1.8
Fine ALSFRS subscore	-	10.3 ± 1.8	9.9 ± 1.9
Gross ALSFRS subscore	-	7.2 ± 1.9	7.4 ± 1.7
Finger Taps/s Right	5.9 ± 1.8	4.2 ± 1.5[a]	3.4 ± 1.2[a]
Finger Taps/s Left	5.8 ± 1.4	3.1 ± 1.5[a]	2.9 ± 1.0[a]
9-Hole peg test Right (s)	21.1 ± 10.2	26.4 ± 8.0[a]	42.1 ± 28.7 [a,b]
9-Hole peg test Left (s)	22.3 ± 9.2	37.2 ± 17.1[a]	42.8 ± 18.1[a]
Resting State fMRI (N)	25	11 8 follow-up	13
Diffusion imaging (N)	28	13 baseline 8 follow-up	18
Thickness measures (N)	27	13 baseline 8 follow-up	18

N= number of participants in each group; number with technically adequate scans

[a] $p < 0.05$ differ from controls, (ANOVA/Tukey's for age; Kruskal-Wallis/Dunn other variables)

[b] $p < 0.05$ Pre-PLS differs from PLS (Mann-Whitney test)